Paper CIT06-1016

FREE CONVECTION INSIDE ANNULAR VERTICAL CONCENTRIC CAVITY: A NEW STRATEGY USING GENERALIZED INTEGRAL TRANSFORM TECHNIQUE

Luiz Mariano Pereira
Universidade Federal do Vale do São Francisco – UNIVASF
Rua da Simpatia, 179, Centro, 56304-440, Petrolina, PE, Brazil
luiz.mariano@univasf.edu.br

Abstract. Free convection inside cavities of annular geometry is a phenomenon present in many engineering devices, reason which is subject of investigation by many researchers. This work deals with free convection heat transfer inside annular vertical concentric cavity using the Generalized Integral Transform Technique – GITT, a hybrid numerical analytical method that has been applied with great success to convection-diffusion problems. This method allows obtaining solution of the governing equations without the necessity of the grid generation requirements. The mathematical formulation of the problem is described by the Navier-Stokes and energy equations in cylindrical coordinates and its representation in streamfunction formulation are adopted. In the present job, the integral transform is first employed in the axial direction and the resulting ordinary differential system to be solved are only a function of the radial coordinate, instead of the previous published paper, which performs the transformation in radial direction. Several values for aspect ratio, thickness between internal and external radii, and Raleigh number are calculated. Results are compared with data available in literature obtained by other numerical methods.

Keywords: Free Convection, Annular Vertical Ducts, GITT

1. Introduction

Free convection inside cavities has received an ever increasing interest of the thermal sciences researchers because of its wide applicability in industrial processes. The precise knowledge of the heat transfer between the cavity walls and the fluid is extremely important in the choice of adequate materials and in the optimum design of thermal equipment. In particular, the flow in the annular region comprehended by circular concentric ducts is of special interest in thermal engineering applications. This flow model occurs, for instance, in double pipe heat exchangers, in nuclear reactors cooling, thermal storage tanks, cylindrical thermal insulation, and various other applications.

The present research intends to add some reference information to the literature by providing results for steady laminar buoyancy induced flow within annular concentric cavities, making use of the Generalized Integral Transform Technique (GITT) (Cotta, 1993; Cotta and Mikhailov, 1997 and Cotta, 1998). In this context, the aim of this work is to illustrate the use of the GITT as a tool in obtaining engineering results for problems of natural convection inside annular concentric vertical cavities, while offering some fully converged benchmark results for future reference.

This class of problems was initially treated by De Vahl Davis and Thomas (1969) and Thomas and De Vahl Davis (1970), who considered natural convection for both vertical annular concentric and rectangular cavities. The problem was modeled by the coupled Navier-Stokes and energy equations, which were then solved using the finite difference method. They investigated the influence of Rayleigh number upon the most relevant heat transfer results. El-Shaarawi and Sarhan (1980), using a boundary layer approach, studied this problem employing the finite difference method. Prasad and Kulacki (1985) developed an experimental apparatus to analyze the natural convection phenomena in a liquid-filled vertical annular cavity, for different heights of the cavity. Kumar and Kalam (1991) also conducted an investigation on this problem, and their results are here recalled for critical comparisons. Aung et al. (1991) and Tsou and Gau (1992) treated the same class of problems but considering the temperature dependence of the fluid properties, and solved it using the finite differences method. Rogers and Yao (1993) undertook the more involved task of performing an instability analysis in vertical annular concentric cavities.

The present analysis is a natural extension in the development of the considered hybrid numerical-analytical approach for heat and fluid flow problems, and some of the more representative previous contributions related to the present work, using the same methodology, can be found in Pereira et al. (1998), Pereira et al. (1999) and Pérez Guerrero at al. (2000).

2. Problem Formulation

The physical problem under consideration is related to an annular concentric vertical cavity closed by two insulated end caps, according to Fig. (1). The annular space is formed by two concentric cylinders with radii R_1 for the internal cylinder wall and R_2 for the external cylinder wall and height Z_{max}. A Newtonian fluid is confined within the cavity and the cylinders walls are maintained at constant and uniform temperatures, with $T_1 > T_2$. The fluid flow is assumed laminar and occurs only by density differences (buoyancy effects) caused by the different side walls

temperatures. Besides, the Boussinesq hypothesis is adopted. The mathematical representation for this problem is given by set of equations: the conservation of mass, momentum and energy, which in steady state and dimensionless form, are written as
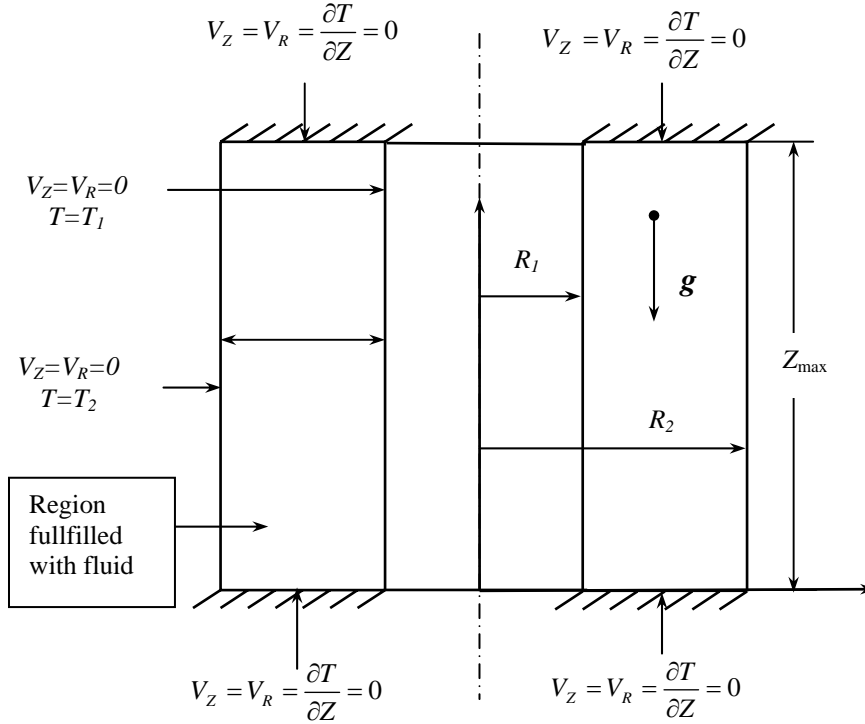

Figure 1. Geometry and coordinates system for natural convection in annular vertical cavities.

$$\frac{\partial v_r}{\partial r} + \frac{v_r}{r} + \frac{\partial v_z}{\partial z} = 0 \tag{1}$$

$$v_r \frac{\partial v_r}{\partial r} + v_z \frac{\partial v_r}{\partial z} = -\frac{\partial p}{\partial r} + Pr\left(\nabla^2 v_r - \frac{v_r}{r^2}\right) \tag{2}$$

$$v_r \frac{\partial v_z}{\partial r} + v_z \frac{\partial v_z}{\partial z} = -\frac{\partial p}{\partial z} + Pr\left(Ra_L \Theta + \nabla^2 v_z\right) \tag{3}$$

$$v_r \frac{\partial \Theta}{\partial r} + v_z \frac{\partial \Theta}{\partial z} = \nabla^2 \Theta \tag{4}$$

and the following dimensionless boundary conditions:

$$\left.\begin{array}{l} v_z = 0 \\ v_r = 0 \\ \Theta = 1 \end{array}\right\}, \quad \text{for } r = r_1 \text{ and } 0 < z < h ; \quad \left.\begin{array}{l} v_z = 0 \\ v_r = 0 \\ \Theta = 0 \end{array}\right\}, \quad \text{for } r = r_2 \text{ and } 0 < z < h \tag{5.a-f}$$

$$\left.\begin{array}{l} v_z = 0 \\ v_r = 0 \\ \dfrac{\partial \Theta}{\partial z} = 0 \end{array}\right\}, \quad \text{for } z = 0 \text{ and } r_1 \le r \le r_2 ; \quad \left.\begin{array}{l} v_z = 0 \\ v_r = 0 \\ \dfrac{\partial \Theta}{\partial z} = 0 \end{array}\right\}, \quad \text{for } z = h \text{ and } r_1 \le r \le r_2 \tag{5.g-l}$$

The dimensionless groups used to write Eqs. (1-4) and the boundary conditions (Eqs. 5), are defined as:

$$v_r = \frac{V_R L}{\alpha} \; ; \; v_z = \frac{V_Z L}{\alpha} \; ; \; r = \frac{R}{L} \; ; \; z = \frac{Z}{L} \; ; \; p = \frac{P}{\rho \alpha^2 / L^2} \; ; \; \Theta = \frac{T - T_2}{T_1 - T_2} \; ; \; Ra_L = \frac{\rho\, g\, \beta (T_1 - T_2) L^3}{\mu \alpha} \; ; \; Pr = \frac{\mu c_p}{k} \tag{6.a-h}$$

where V_R and V_Z are the dimensional radial and axial velocity components, respectively; R and Z are the dimensional radial and axial coordinates, respectively; P is the dimensional absolute pressure; T is the dimensional absolute

temperature; T_1 and T_2 are related to the dimensional absolute temperatures of the internal and external cylinders walls; g is the gravity acceleration; α is the thermal diffusivity; ρ is the specific mass; β is the thermal expansion coefficient; μ is the absolute viscosity; c_p is the specific heat at constant pressure; k is the fluid thermal conductivity; Ra_L is the Rayleigh number, based on the cavity width; and Pr is the Prandtl number. The following additional dimensionless parameters are then defined:

$$r_1 = \frac{R_1}{L} ; \quad r_2 = \frac{R_2}{L} ; \quad \varpi = \frac{r_2}{r_1} ; \quad L = R_2 - R_1 ; \quad h = \frac{Z_{máx}}{L} \qquad (6.\text{i-m})$$

with r_1 and r_2 being the dimensionless positions of the internal and external cylinders walls, respectively; ϖ is the radii ratio; L is the cavity width and h is the ratio between the height and width of the cavity (aspect ratio).

The momentum equations can be represented in the streamfunction-only formulation to eliminate the pressure terms and automatically satisfy the continuity equation. Therefore, using the same procedure adopted by Pereira et al. (1998), the following dimensionless coupled partial differential equations are generated:

$$E^4\psi = \frac{1}{P_r}\left[\frac{1}{r}\frac{\partial\psi}{\partial z}\frac{\partial(E^2\psi)}{\partial r} - \frac{1}{r}\frac{\partial\psi}{\partial r}\frac{\partial(E^2\psi)}{\partial z} - \frac{2}{r^2}\frac{\partial\psi}{\partial z}E^2\psi\right] + Ra_L\frac{\partial\Theta}{\partial r}, \quad for \quad \begin{cases} r_1 < r < r_2 \\ 0 < z < h \end{cases} \qquad (7.\text{a})$$

$$\nabla^2\Theta = \frac{1}{r}\frac{\partial\psi}{\partial z}\frac{\partial\Theta}{\partial r} - \frac{1}{r}\frac{\partial\psi}{\partial r}\frac{\partial\Theta}{\partial z}, \quad for \quad \begin{cases} r_1 < r < r_2 \\ 0 < z < h \end{cases} \qquad (7.\text{b})$$

with boundary conditions:

$$\left.\begin{array}{l} \psi = 0 \\ \dfrac{\partial\psi}{\partial r} = 0 \\ \Theta = 1 \end{array}\right\}, \quad for \quad r = r_1 \qquad\qquad \left.\begin{array}{l} \psi = 0 \\ \dfrac{\partial\psi}{\partial r} = 0 \\ \Theta = 0 \end{array}\right\}, \quad for \quad r = r_2 \qquad (7.\text{c-h})$$

$$\left.\begin{array}{l} \psi = 0 \\ \dfrac{\partial\psi}{\partial z} = 0 \\ \dfrac{\partial\Theta}{\partial z} = 0 \end{array}\right\}, \quad for \quad z = 0 \qquad\qquad \left.\begin{array}{l} \psi = 0 \\ \dfrac{\partial\psi}{\partial z} = 0 \\ \dfrac{\partial\Theta}{\partial z} = 0 \end{array}\right\}, \quad for \quad z = h \qquad (7.\text{i-n})$$

where

$$E^2 \equiv \frac{\partial^2}{\partial r^2} - \frac{1}{r}\frac{\partial}{\partial r} + \frac{\partial^2}{\partial z^2} \qquad (7.\text{o})$$

$$E^4\psi = E^2(E^2\psi) \qquad (7.\text{p})$$

The fact that no flow occurs across the boundaries of the cavity, makes it possible to take $\psi = 0$ without loss of generality. Therefore, all the boundary conditions at radial and axial directions become homogeneous.

2.1 Solution Methodology

According to the integral transformation approach, the first step is to choose auxiliary eigenvalue problems for the momentum and energy equations. Due the homogeneous nature of the axial boundary conditions, the forth order eigenvalue problem used by Pérez-Guerrero et al. (1999) was here employed as the auxiliary problem to solve the streamfunction equation, which is written as

$$\frac{d^4 X_i(z)}{dz^4} = \gamma_i^4 X_i(z), \quad for \quad 0 < z < h \qquad (8.\text{a})$$

$$\left.\begin{array}{l} X_i = 0 \\ \dfrac{dX_i}{dz} = 0 \end{array}\right\}, \quad \text{at } z = 0 ; \qquad \left.\begin{array}{l} X_i = 0 \\ \dfrac{dX_i}{dz} = 0 \end{array}\right\}, \quad \text{at } z = h \tag{8.b-e}$$

where $X_i(z)$ and γ_i are the eigenfunctions and eigenvalues, respectively.

The solution is shown in details in Pérez-Guerrero (1999) and its general form is

$$X_i(z) = \begin{cases} \dfrac{Cos\left[(z-\frac{h}{2})\gamma_i\right]}{Cos(\gamma_i \frac{h}{2})} - \dfrac{Cosh\left[(z-\frac{h}{2})\gamma_i\right]}{Cosh(\gamma_i \frac{h}{2})}, & for \quad i \quad odd \\[4mm] \dfrac{Sin\left[(z-\frac{h}{2})\gamma_i\right]}{Sin(\gamma_i \frac{h}{2})} - \dfrac{Sinh\left[(z-\frac{h}{2})\gamma_i\right]}{Sinh(\gamma_i \frac{h}{2})}, & for \quad i \quad even \end{cases} \tag{8.f}$$

Orthogonality property

$$\int_0^h X_i(z) X_j(z)\, dz = \begin{cases} 0, & if \quad i \neq j \\ N_i, & if \quad i = j \end{cases} \tag{9.a}$$

The eigenvalues γ_i´s are the roots of the following transcendental equation

$$Cosh(\gamma_i \tfrac{h}{2}) = Sec(\gamma_i \tfrac{h}{2}) \tag{9.b}$$

In the case of the energy equation, the auxiliary problem for the energy equation is of the Sturm-Liouville type, written as:

$$\frac{d^2\Gamma_m(z)}{dz^2} + \lambda_m^2 \Gamma_m(z) = 0, \quad for \quad 0 < z < h, \quad m=1,2,3,... \tag{10.a}$$

$$\left.\frac{d\Gamma_m}{dz}\right|_{z=0} = 0 ; \qquad \left.\frac{d\Gamma_m}{dz}\right|_{z=h} = 0 \tag{10.b,c}$$

where $\Gamma_m(z)$ and λ_m are the eigenfunctions and the eigenvalues, respectively.

The solution of this auxiliary problem are readily available in Ozisik (1993) and given by

$$\Gamma_m(z) = Cos(\lambda_m z) \tag{10.d}$$

and the engenvalues are

$$\lambda_m = (m-1)\pi, \quad for \quad m = 1,2,3,... \tag{10.e}$$

note that $\lambda_0 = 0$ is a eigenvalue too.

The eigenfunctions obey the following ortoghonality property

$$\int_0^h \Gamma_m(z)\Gamma_n(z)\, dz = \begin{cases} 0, & if \quad m \neq n \\ M_m, & if \quad m = n \end{cases} \tag{10.f}$$

2.2 The Integral Transform Pairs

The next step in the solution procedure is to determine the integral transform pairs. Making use of the orthogonality properties of the eigenfunctions, the following integral transform pairs for the streamfunction and temperature equations are obtained, respectively:

$$\overline{\psi}_i(r) = \int_0^h \tilde{X}_i(z)\,\psi(r,z)\,dz\,, \qquad \text{(transform)} \tag{11.a}$$

$$\psi(r,z) = \sum_{i=1}^\infty \tilde{X}_i(z)\,\overline{\psi}_i(r)\,, \qquad \text{(inversion)} \tag{11.b}$$

$$\overline{\Theta}_m(r) = \int_0^h \tilde{\Gamma}_m(z)\,\Theta(r,z)\,dz\,, \qquad \text{(transform)} \tag{12.a}$$

$$\Theta(r,z) = \sum_{m=1}^\infty \tilde{\Gamma}_m(z)\,\overline{\Theta}_m(r)\,, \qquad \text{(inversion)} \tag{12.b}$$

where the symbol '~' represents the normalized eigenfunctions which are written as

$$\tilde{X}_i(z) = \frac{X_i(z)}{\sqrt{N_i}}\,; \qquad\qquad \tilde{\Gamma}_m(z) = \frac{\Gamma_m(z)}{\sqrt{M_m}} \tag{12.c,d}$$

2.3 The Ordinary Differential Systems

Using the transformation rules, given by Eqs. (11-12), the coupled partial differential equations with their respective boundary conditions are transformed resulting in the following ordinary differential systems:

$$\frac{d^4\overline{\psi}_i(r)}{dr^4} = -\gamma_i^4\overline{\psi}_i + \frac{3}{r^3}\frac{d\overline{\psi}_i}{dr} - \frac{3}{r^2}\frac{d^2\overline{\psi}_i}{dr^2} + \frac{2}{r}\frac{d^3\overline{\psi}_i}{dr^3} + \sum_{j=1}^\infty 2A_{ij}\left(\frac{1}{r}\frac{d\overline{\psi}_i}{dr} - \frac{d^2\overline{\psi}_i}{dr^2}\right) +$$

$$\frac{1}{rP_r}\left[A_{ijk}\left(\overline{\psi}_j\frac{d^3\overline{\psi}_k}{dr^3} + \frac{3}{r^2}\overline{\psi}_j\frac{d\overline{\psi}_k}{dr} - \frac{3}{r}\overline{\psi}_j\frac{d^2\overline{\psi}_k}{dr^2} - \frac{d^2\overline{\psi}_j}{dr^2}\frac{d\overline{\psi}_k}{dr} + \frac{1}{r}\frac{d\overline{\psi}_j}{dr}\frac{d\overline{\psi}_k}{dr}\right) +$$

$$B_{ijk}\left(\overline{\psi}_j\frac{d\overline{\psi}_k}{dr} - \frac{2}{r}\overline{\psi}_j\overline{\psi}_k\right) - C_{ijk}\left(\frac{d\overline{\psi}_j}{dr}\overline{\psi}_k\right)\right] + R_{aL}B_{im}\frac{d\overline{\Theta}_m}{dz} \tag{13.a}$$

$$\frac{d^2\overline{\Theta}_m(r)}{dr^2} = \lambda_m^2\overline{\Theta}_m - \frac{1}{r}\frac{d\overline{\Theta}_m}{dr} + \frac{1}{r}\sum_{n=1}^\infty\sum_{j=1}^\infty\left(E_{mnj}\frac{d\overline{\Theta}_m}{dr}\overline{\psi}_j - F_{mnj}\overline{\Theta}_m\frac{d\overline{\psi}_j}{dr}\right) \tag{14.a}$$

with the following radial boundary conditions

$$\overline{\psi}_i(r_1) = 0\,; \quad \left.\frac{d\overline{\psi}_i}{dr}\right|_{r=r_1} = 0\,; \quad \overline{\psi}_i(r_2) = 0\,; \quad \left.\frac{d\overline{\psi}_i}{dr}\right|_{r=r_2} = 0 \tag{13.b-e}$$

$$\overline{\Theta}_m(r_1) = 0\,; \quad \overline{\Theta}_m(r_2) = \begin{cases} h/\sqrt{M_m}\,, & \text{if} \quad m=1 \\ 0\,, & \text{if} \quad m>1 \end{cases} \tag{14.b,c}$$

The coefficients A_{ij}, A_{ijk}, B_{ijk}, C_{ijk}, B_{im}, E_{mnj} and F_{mnj} appearing in Eqs. (13.a and 14.a), which result from the integral transformation procedure, are defined as (Pereira, 2000):

$$A_{ij} = \int_0^h\left(\tilde{X}_i\frac{d^2\tilde{X}_j}{dz^2}\right)dz\,; \tag{15.a}$$

$$A_{ijk} = \int_0^h\left(\tilde{X}_i\frac{d\tilde{X}_j}{dz}\tilde{X}_k\right)dz\,; \tag{15.b}$$

$$B_{ijk} = \int_0^h\left(\tilde{X}_i\frac{d\tilde{X}_j}{dz}\frac{d^2\tilde{X}_k}{dz^2}\right)dz\,; \tag{15.c}$$

$$C_{ijk} = \int_0^h \left(\tilde{X}_i \frac{d^3 \tilde{X}_j}{dz^3} \tilde{X}_k \right) dz ; \qquad (15.d)$$

$$E_{mnj} = \int_0^h \left(\tilde{\Gamma}_m \tilde{\Gamma}_n \frac{d\tilde{X}_j}{dz} \right) dz ; \qquad (15.e)$$

$$B_{mnj} = \int_0^h \left(\tilde{\Gamma}_m \frac{d\tilde{\Gamma}_n}{dz} \tilde{X}_j \right) dz \qquad (15.f))$$

$$B_{im} = \int_0^h \left(\tilde{X}_i \tilde{\Gamma}_m \right) dz \qquad (15.g)$$

3. Results and Discussion

The resulting fourth order and second order ordinary differential system for streamfunction and temperature, respectively, joint with the boundary conditions are solved through the subroutine BVPFD (IMSL Library, 1989) which is appropriate to solve this kind of problems under a user prescribed error target, here taking as 10^{-4} for the transformed streamfunction and temperature potentials.

Table 1. Convergence of streamfunction and temperature for P_r=0.7, h=1, ϖ=2, R_{aL}=10^5, and various r and z positions.

	$\psi(r,z)$			$\Theta(r,z)$		
NT	r =1.1	**1.5**	**1.9**	r =1.1	**1.5**	**1.9**
		$z = 0.1$			$z = 0.1$	
20	-0.1794E+01	-0.1995E+01	-0.9060E+00	0.3330E+00	0.1370E+00	0.5235E-01
24	-0.1794E+01	-0.1995E+01	-0.9059E+00	0.3338E+00	0.1370E+00	0.5232E-01
26	-0.1795E+01	-0.1995E+01	-0.9059E+00	0.3338E+00	0.1370E+00	0.5231E-01
28	-0.1795E+01	-0.1995E+01	-0.9060E+00	0.3337E+00	0.1370E+00	0.5230E-01
30	-0.1796E+01	-0.1995E+01	-0.9061E+00	0.3336E+00	0.1370E+00	0.5229E-01
		$z = 0.5$			$z = 0.5$	
20	-0.6091E+01	-0.1189E+02	-0.5945E+01	0.5035E+00	0.3589E+00	0.2639E+00
24	-0.6091E+01	-0.1189E+02	-0.5945E+01	0.5036E+00	0.3589E+00	0.2638E+00
26	-0.6092E+01	-0.1189E+02	-0.5946E+01	0.5037E+00	0.3589E+00	0.2637E+00
28	-0.6091E+01	-0.1189E+02	-0.5946E+01	0.5036E+00	0.3589E+00	0.2638E+00
		$z = 0.9$			$z = 0.9$	
20	-0.1793E+01	-0.2977E+01	-0.2028E+01	0.8410E+00	0.7057E+00	0.4463E+00
24	-0.1793E+01	-0.2977E+01	-0.2028E+01	0.8409E+00	0.7057E+00	0.4458E+00
26	-0.1793E+01	-0.2977E+01	-0.2029E+01	0.8409E+00	0.7057E+00	0.4458E+00
28	-0.1794E+01	-0.2977E+01	-0.2030E+01	0.8409E+00	0.7057E+00	0.4458E+00
30	-0.1794E+01	-0.2977E+01	-0.2030E+01	0.8409E+00	0.7057E+00	0.4459E+00

In table (1) is showed the convergence behavior for both streamfunction and temperature profiles. It is considered several radial and axial positions within the annular space and the values R_{aL}=10^5 and P_r=0.7 was applied. It can be noticed that close to the edges of the cavity, corresponding to the region of greater gradient, the convergence was attained with higher truncation orders in the expansions, as expected. For all considered positions, a maximum number of terms, such as NT=30, in the streamfunction and temperature inversion formulae was required to achieve full convergence to four significant digits. With the increase of the Rayleigh number, the convergence rates of the eigenfunction expansions, for both the streamfunction and the temperature, are also affected, due to the dominance of convective effects. This behavior is more noticeable in regions closer to the inner and outer walls of the cavity, due the gradients are more pronounced. On the other hand, at the vertical mid plane of the cavity (r = 1.5) only a few terms are necessary for the convergence.
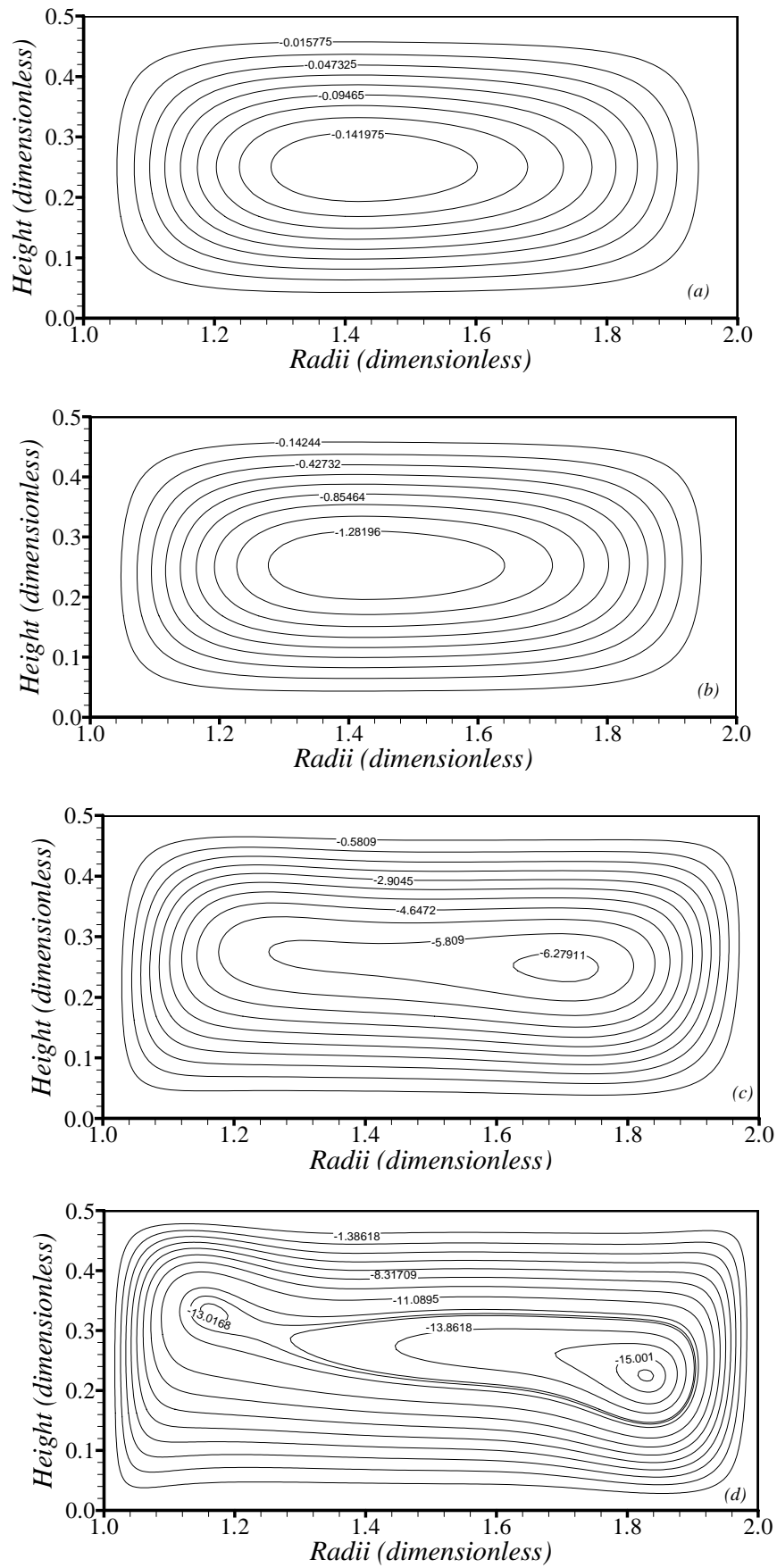
Figure 2. Streamfunction for Pr=0.7, ϖ=2.0 h = 0.5 for: (a) Ra_L=10^3; (b) Ra_L=10^4; (c) Ra_L=10^5 and (d) Ra_L=10^6.

Figures (2.a-d) show the isolines of streamfunction for $\varpi = 2.0$ and $h=0.5$ and various values of the parameter Ra_L. It is worth recalling that in the case of $Ra_L=10^3$ and 10^4 (Figs. 2.(a) and (b)), only one vortex is detected, with an elliptical shape and located at the cavity center, which is deformed when Ra_L increases. When Ra_L increases, a secondary vortex arise at left hand upper side of the cavity. This vortex is more pronounced in the case of $Ra_L=10^6$. In this case, the temperature isolines are almost parallel, showing the dominance of the conductive heat transfer process inside the cavity for low Rayleigh number.

According to Fig. (2.b) for $Ra_L=10^5$, $h=1$ and $\varpi=2$, a secondary vortex is observed above the axial primary vortex. It is also is observed in Fig. (2.b) that the isolines of the temperature field collapse at the bottom of the hot and cold walls, turning the boundary layers much finer with the increase in Ra_L, as can further observed in Fig. (2.c) for the case $Ra_L=10^6$.

The case of a cavity with $h=5$ and $Ra_L=10^5$ is illustrated in Fig. (3). It should be noted that with the increase of the aspect ratio, the structure of the vortices is modified. The behavior of the isolines, Figs. (2-3), for both steamfunction and temperature, shows a reasonable graphical agreement with other results reported in the literature (De Vahl Davis and Thomas, 1969, Thomas and De Vahl Davis, 1970, Kumar and Kalam, 1991, and Kumar, 1997).
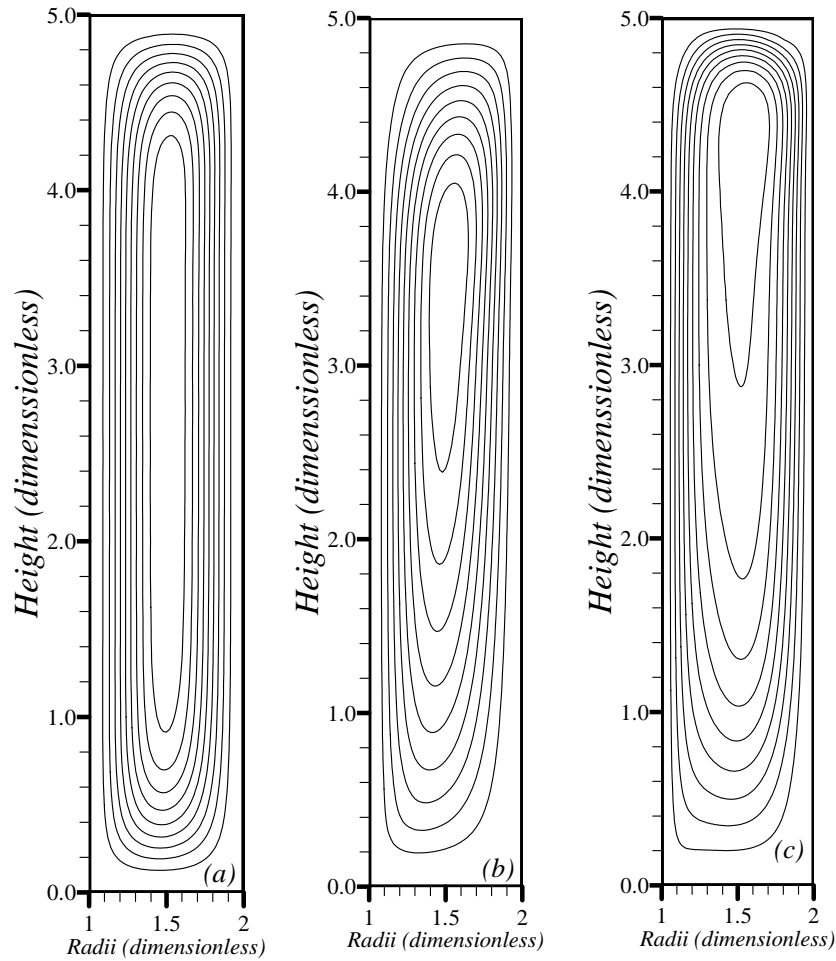

Figure 3. Isolines of streamfunction for *Pr*=0.7, $\varpi=2.0$ *h* = 5.0 for: (a) $Ra_L=10^3$; (b) $Ra_L=10^4$; and (c) $Ra_L=10^5$.

The local Nusselt Number was obtained by the use of the following definition:

$$Nu_w = -\frac{\partial \Theta}{\partial r}\bigg|_{r=r_w} \text{, with } w = \begin{cases} 1 & \text{for internal cylinder wall} \\ 2 & \text{for external cylinder wall} \end{cases} \tag{16}$$

The average Nusselt number is calculated through the integration of the local Nusselt number along the cavity height, as:

$$\overline{Nu}_{w} = \frac{1}{h} \int_{0}^{h} Nu_{w} \, dz \tag{17}$$

Results for the average Nusselt number, evaluated at the internal wall ($\overline{Nu}_1$), are presented in Tab. (2) for aspect ratios $h=1$ and 5 and for radii ratios $\varpi=2.0$ and 5.0. The Rayleigh number is varied from 10^2 to 10^6 so as to illustrate its influence on the Nusselt number convergence behavior. It can be observed that for the majority of the selected cases (except for $Ra_L=10^6$, $h=1$ and $\varpi=2.0$) the convergence is achieved with four significant digits for NT<40 for the expansions truncation.

Figure (4) shows the variation of Nusselt number along the inner (Nu_1) and outer (Nu_2) cavity walls, for $Pr=0.7$, $h=1$, $Ra_L=10^5$, $\varpi=2$ and 5, calculated with NT = 40 terms in both expansions. It is observed in Fig. (4.a) that the heat transfer rate is increased in the lower region of the hot wall (inner wall) for the proposed variation in ϖ. In Fig. (4.b) for the outer wall, the rate of heat transfer decreases with the increase in ϖ. In Fig. (5) a comparison is made between the present results and those obtained by Kumar and Kalam (1991), for the average Nusselt number at the inner wall. There is a reasonable agreement between the two sets of result, while the small difference between them could still be due to differences in the local Nusselt number definition, which is not presented in Kumar and Kalam (1991).
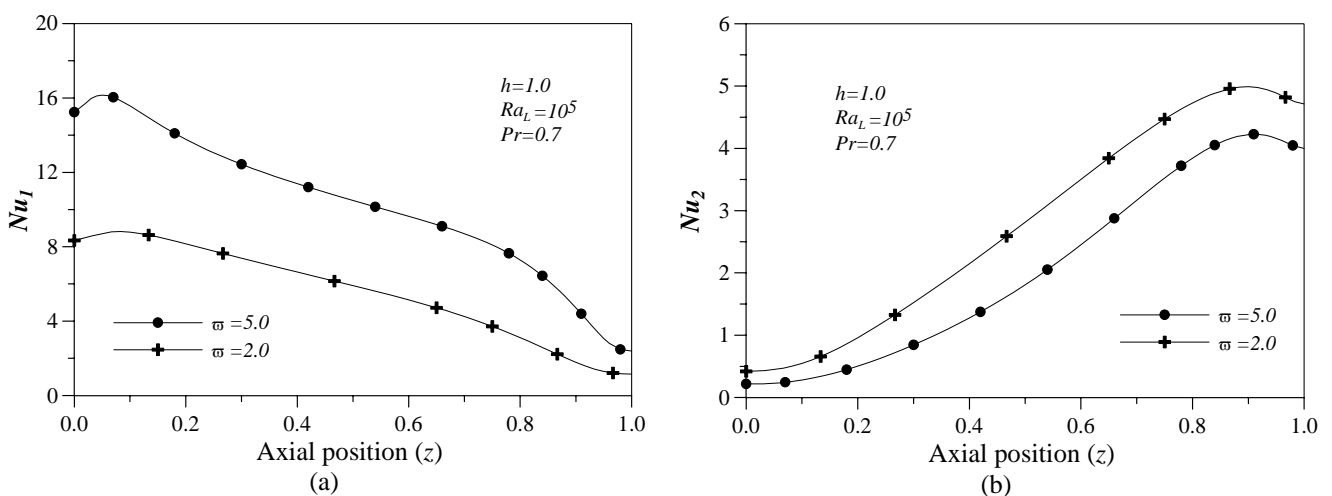

Figure 4. Axial local Nusselt number behavior (Nu_w) for $Pr=0.7$, $h=1$ and $Ra_L=10^5$ at: (a) inner wall; (b) outer wall.
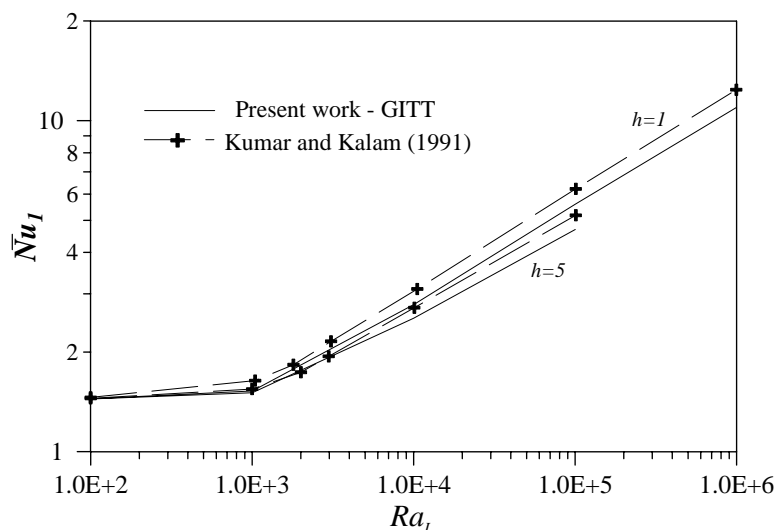

Figure 5. Average Nusselt number at the inner wall against Ra_L, for $Pr = 0.7$, $\varpi = 2.0$ and different values of h.

4. Concluding Remarks

The Generalized Integral Transform Technique is successfully implemented for the hybrid solution of natural convection within vertical concentric annular cavities, under laminar and steady flow conditions. A set of reference results with global error control is provided, in both tabular and graphical formats, and previously reported results from discrete approaches are critically examined and covalidated. These encouraging results allow now for the extension of the present analysis towards more involved situations, including variable thermophysical fluid properties.

5. Acknowledgements

6. References

Aung, W., Moghadam, H. E. and Tsou, F. K., 1991 "Simultaneous Hydrodynamic and Thermal Development in Mixed Convection in a Vertical Annulus with Fluid Property Variations", Trans. ASME – J. Heat Transfer, 113, pp. 926-931.

Cotta, R. M., 1993, "Integral Transforms in Computational Heat and Fluid Flow", Boca Raton, FL, CRC Press.

Cotta, R. M. and Mikhailov, M. D., 1997, "Heat Conduction – Lumped Analysis, Integral Transforms, Symbolic Computation", John Wiley & Sons, Chichester, England.

Cotta, R. M., 1998, "The Integral Transform Method in Thermal & Fluids Sciences & Engineering", N. Y., Begell House.

De Vahl Davis, G. and Thomas, R. W., 1969, "Natural Convection Between Concentric Vertical Cylinders", Physics of Fluids, Supl. II, pp. 198-207.

El-Shaarawi, M. A. I. and Sarhan, A., 1980, "Free Convection Effects on the Developing Laminar Flow in Vertical Concentric Annuli", Trans. ASME – J. Heat Transfer, Vol. 102, pp. 617-622.

IMSL Library, 1989, Math/Lib., Houston, Texas.

Kumar, R. and Kalam, M. A., 1991, "Laminar Thermal Convection Between Vertical Coaxial Isothermal Cylinders", Int. J. Heat Mass Transfer, Vol. 34(2), pp. 513-524.

Ozisik, M. N., 1993, "Heat Conduction", 2nd ed., N. Y., John Wiley & Sons.

Pereira, L. M., Cotta, R. M. and Pérez Guerrero, J. S., 1999, "Analysis of Laminar Forced Convection in Annular Ducts Using Integral Transforms", Proc. of the 15th Brazilian Congress of Mechanical Engineering, COBEM 99, Águas de Lindóia, São Paulo, Brazil, December, (CD-ROM); also, Hybrid Meth. Eng., Vol. 2(2), pp. 221-232, 2000.

Pérez Guerrero, J. S., Quaresma, J. N. N. and Cotta, R. M., 2000, "Simulation of Laminar Flow Inside Ducts of Irregular Geometry Using Integral Transforms", Computational Mechanics, Vol. 25, pp. 413-420.

Prasad, V. and Kulacki, F. A., 1985, "Free Convective Heat Transfer in a Liquid-Filled Vertical Annulus", Trans. ASME – J. Heat Transfer, Vol. 107, pp. 596-602.

Rogers, B. B. and Yao, L.S., 1993, "Natural Convection in a Heated Annulus", Int. J. Heat Mass Transfer, Vol. 36(1), pp. 35-47.

Tsou, F. K. and Gau, C., 1992, "Wall Heating Effects in Mixed Convection in Vertical Annulus with Variable Properties", J. Thermophysics and Heat Transfer, Vol. 6, pp. 273-276.